J|A|C|S
ARTICLES
Published on Web 04/07/2007

Lamellar Structure in Poly(Ala-Gly) Determined by Solid-State NMR and Statistical Mechanical Calculations

Tetsuo Asakura,* Hirohiko Sato, Fumika Moro, Yasumoto Nakazawa, and Akihiro Aoki

Contribution from the Department of Biotechnology, Tokyo University of Agriculture and Technology, Koganei, Tokyo 184-8588, Japan

Received January 8, 2007; E-mail: asakura@cc.tuat.ac.jp

Abstract: Lamellar structure of poly(Ala-Gly) or $(AG)_n$ in the solid was examined using ^{13}C solid-state NMR and statistical mechanical approaches. Two doubly labeled versions, [1-^{13}C]Gly^{14}[1-^{13}C]Ala^{15}- and [1-^{13}C]-Gly^{18}[1-^{13}C]Ala^{19} of $(AG)_{15}$ were examined by two-dimensional (2D) ^{13}C spin diffusion NMR in the solid state. In addition five doubly labeled [^{15}N,^{13}C]-versions of the same peptide, $(AG)_{15}$ and 15 versions labeled [3-^{13}C] in each of the successive Ala residues were utilized for REDOR and ^{13}C CP/MAS NMR measurements, respectively. The observed spin diffusion NMR spectra were consistent with a structure containing a combination of distorted β-turns with a large distribution of the torsion angles and antiparallel β-sheets. The relative proportion of the distorted β-turn form was evaluated by examination of ^{13}C CP/MAS NMR spectra of [3-^{13}C]Ala-$(AG)_{15}$. In addition, REDOR determinations showed five kinds of atomic distances between doubly labeled ^{13}C and ^{15}N nuclei which were also interpreted in terms of a combination of β-sheets and β-turns. Our statistical mechanical analysis is in excellent agreement with our Ala Cβ ^{13}C CP/MAS NMR data strongly suggesting that $(AG)_{15}$ has a lamellar structure.

Introduction

Silk fibroin from *Bombyx mori* silkworm has outstanding mechanical properties such as exceptional strength and toughness, despite being spun from aqueous solution.[1] Two distinct structures in the solid state, silk I before spinning and silk II after spinning, have been proposed on the basis of X-ray fiber diffraction, conformational energy calculations, infrared spectroscopy, and solid-state NMR.[2] The conformation of silk I has been shown by us to have a repeated type-II β-turn structure with the use of solid-state NMR approaches such as two-dimensional (2D) spin diffusion NMR under off magic angle spinning, rotational echo double resonance (REDOR), and ^{13}C chemical shift data as well as X-ray diffraction analysis.[2,3]

On the other hand, the conformation of silk II was characterized first by Marsh et al.[4] as an antiparallel β-sheet based on a fiber X-ray diffraction study of native *B. mori* silk fiber. Later, Fraser et al.,[5] Lotz and Keith,[6] and Fossey et al.[7] supported the general features of this antiparallel β-sheet model, although some disordered structure is also present in the silk fibers. Takahashi et al.[8] reported a more detailed X-ray fiber diffraction analysis of *B. mori* silk fibroin based on 35 quantified intensities. After considering the previously proposed models for silk II in terms of the experimentally derived *R* factor, these authors[8] proposed that two antipolar, antiparallel β-sheet structures are statistically stacked with different orientations, occupying the crystal site with a ratio of 1:2. In these structural studies of *B. mori* silk fibroin, $(AG)_n$ has been used as a pertinent model system for NMR studies, because the primary structure of *B. mori* silk contains multiple repeats of $(AGSGAG)_n$ which make up 55% of the total fiber and form the insoluble quasi-crystalline Cp-fraction after chymotrypsin cleavage.[1] The chain-folded lamellar structure has been proposed for $(AG)_{64}$ in the silk II form[9] and, on the basis of SAN and WAX scattering,[10] for a dried hydrogel of regenerated silk fibroin slowly converted to a silk II structure.

Solid-state NMR is useful for determining the silk I structure and has also been used to clarify the silk II structure of $(AG)_{15}$.[11,12] Broad and asymmetric Ala Cβ peaks were observed in the CP/MAS NMR spectra of $(AG)_{15}$, indicating a heterogeneous structure[11,12] in contrast to the singly ordered secondary structure of silk I. The relative proportions of the various heterogeneous components were determined from their relative peak intensities of the deconvoluted line shape.[5] For example, the deconvoluted Ala Cβ peaks of $(AG)_{15}$ yielded 27% *distorted*

(1) Asakura, T.; Kaplan, D. L. In *Encyclopedia of Agricultural Science*; Arutzen, C. J., Ed.; Academic Press: New York, 1994; Vol. 4, pp 1−11.
(2) Asakura, T.; Ohgo, K.; Komatsu, K., Kanenari, M.; Okuyama, K. *Macromolecules* **2005**, *38*, 7397−7403 and references therein.
(3) Asakura, T.; Ashida, J.; Yamane, T.; Kameda, T.; Nakazawa, Y.; Ohgo K.; Komatsu K. *J. Mol. Biol.* **2001**, *306*, 291−305.
(4) Marsh, R.; Corey, R. B.; Pauling, L. *Biochem. Biophys. Acta* **1955**, *16*, 1−34.
(5) Fraser, B.; MacRae, T. P. *Conformations of Fibrous Proteins and Related Synthetic Polypeptides*; Academic Press: New York, 1973.
(6) Lotz, B.; Keith, H. D. *J. Mol. Biol.* **1971**, *61*, 201−215.
(7) Fossey, S. A.; Nemethy, G.; Gibson, K. D.; Scheraga, H. A. *Biopolymers* **1991**, *31* 1529−1541.
(8) Takahashi, Y.; Gehoh, M.; Yuzuriha, K. *Int. J. Biol. Macromol.* **1999**, *24*, 127−138.
(9) Panitch, A.; Matsuki, K.; Cantor, E. J.; Cooper, S. J.; Atkins, E. D. T.; Fournier, M. J.; Mason, T. L.; Tirrell, D. A. *Macromolecules* **1997**, *30*, 42−49.
(10) Valluzzi, R.; Jin, H. J. *Biomacromolecules* **2004**, *5*, 696−703.
(11) Asakura, T.; Yao, J.; Yamane, T.; Umemura, K.; Ulrich, A. S. *J. Am. Chem. Soc.* **2002**, *124*, 8794−8795.
(12) Asakura, T.; Yao, J. *Protein Sci.* **2002**, *11*, 2706−2713.

β-turn(16.7 ppm), 46% β-sheet (alternating Ala residues)(19.1 ppm), and 27% β-sheet (parallel Ala residues)(22.4 pppm). Recently, ^{13}C solid-state NMR on selectively ^{13}C-labeled peptides labeled singly at different Ala methyl carbons was used to examine the silk II structure of $(AG)_{15}$ with emphasis on a possible lamellar structure containing β-turns.[13]

In the present paper, we used solid-state NMR approaches such as 2D spin diffusion, under off magic angle spinning and REDOR NMR, and ^{13}C chemical shift contour plots of the Cβ carbon of Ala residue to study in detail the structure for $(AG)_{15}$ in silk II form, supported by statistical mechanical calculations for $(AG)_{15}$.

Experimental Section

Sample Preparations. Using solid-phase Fmoc-chemistry, we prepared two ^{13}C doubly labeled peptides of $(AG)_{15}$: $(AG)_6A[1\text{-}^{13}C]\text{-}G^{14}[1\text{-}^{13}C]A^{15}G(AG)_7$ and $(AG)_8A[1\text{-}^{13}C]G^{18}[1\text{-}^{13}C]A^{19}G(AG)_5$ for 2D spin diffusion NMR experiments; five ^{13}C,^{15}N-labeled peptides of $(AG)_{15}$: (D1) $(AG)_7[^{15}N]A^{15}[2\text{-}^{13}C]G^{16}(AG)_7$, (D2) $(AG)_7A[^{15}N]Gly^{16}[2\text{-}^{13}C]Ala^{17}G(AG)_6$, (D3) $(AG)_6A[1\text{-}^{13}C]Gly^{14}A[^{15}N]Gly^{16}(AG)_7$, (D4) $(AG)_7[1\text{-}^{13}C]Ala^{15}G[^{15}N]Ala^{17}G(AG)_6$, and (D5) $(AG)_7[^{15}N]Ala^{15}[1\text{-}^{13}C]\text{-}Gly^{16}(AG)_7$ for REDOR analysis, and 15 [3-^{13}C]A-singly labeled versions of the same peptide with different labeling positions and $(AG)_{25}$ for CP/MAS NMR. A fully automated Pioneer Peptide Synthesis System (Applied Biosystem Ltd.)[2] was used throughout. MALDI-TOFMS (Applied Biosystem Ltd.) was used to characterize $(AG)_{15}$ peptide. After synthesis the samples were dissolved in formic acid and thoroughly dried before use in NMR experiments. Their purity of $(AG)_{15}$ was more than 90%, and the structure was predominantly β-sheet as determined from the ^{13}C CP/MAS NMR spectra.[11]

^{13}C CP/MAS NMR Measurements. ^{13}C CP/MAS NMR experiments[14] were performed on a Chemagnetics Infinity 400 MHz spectrometer with an operating frequency of 100.0 MHz for ^{13}C at a sample spinning rate of 10 kHz (a 4-mm diameter Zr rotor). Number of acquisitions was 8000, and the recycle delay was 5 s. A 50 kHz radio frequency field strength was used for ^{1}H$-^{13}$C decoupling with the acquisition period of 12.8 ms. A 90° pulse width of 5 μs with 1 ms CP contact time was employed. Phase cycling was used to minimize artifacts. ^{13}C chemical shifts were calibrated indirectly through the adamantane methylene peak observed at 28.8 ppm relative to TMS (tetramethylsilane) at 0 ppm.[2]

2D Spin Diffusion ^{13}C Solid-State NMR Measurements. The 2D spin diffusion NMR spectra were observed using a Varian Unity *INOVA* 400 NMR spectrometer with a 7-mm Jakobsen-type double-tuned MAS probe at off magic angle condition ($\theta_m-7°$) at room temperature.[13] The sample spinning rate was 6 kHz ($\pm$3 Hz). The scaling factor of the 2D spin diffusion spectra is $1/2\ (3\cos^2(\theta_m - 7°) - 1) = 0.198$. The mixing times were set to 2s. The contact time was set to 2 ms using the variable-amplitude CP technique. About 400 scans with a recycle delay of 2 s were accumulated for every T_1 value in the 2D experiment. The principal values of the chemical shift tensors for the carbonyl carbon nuclei of the ^{13}C-labeled Ala and Gly residues were determined by analysis of the spinning sidebands under slow MAS conditions using a Chemagnetics Infinity 400 spectrometer.[3]

REDOR Measurements. The REDOR experiments[15,16] were performed on a Chemagnetics Infinity 400 MHz spectrometer (100.0 MHz for ^{13}C and 40.3 MHz for ^{15}N) using the following conditions:[17] a 4-mm triple-channel magic-angle probe; spinning rate 6.7 kHz; 180° pulses for ^{13}C and ^{15}N channels respectively of 6.5 and 8.2 μs duration; recycle delay of 3 s. Phases of ^{15}N 180° pulses were cycled according to the XY-8 scheme[3] to minimize off-resonance and pulse error effects. REDOR evolution times ranged up to 18 ms. Values of $\Delta S/S_0 = 1 - S/S_0$ were computed as the ratios of peak intensities in the REDOR spectra.

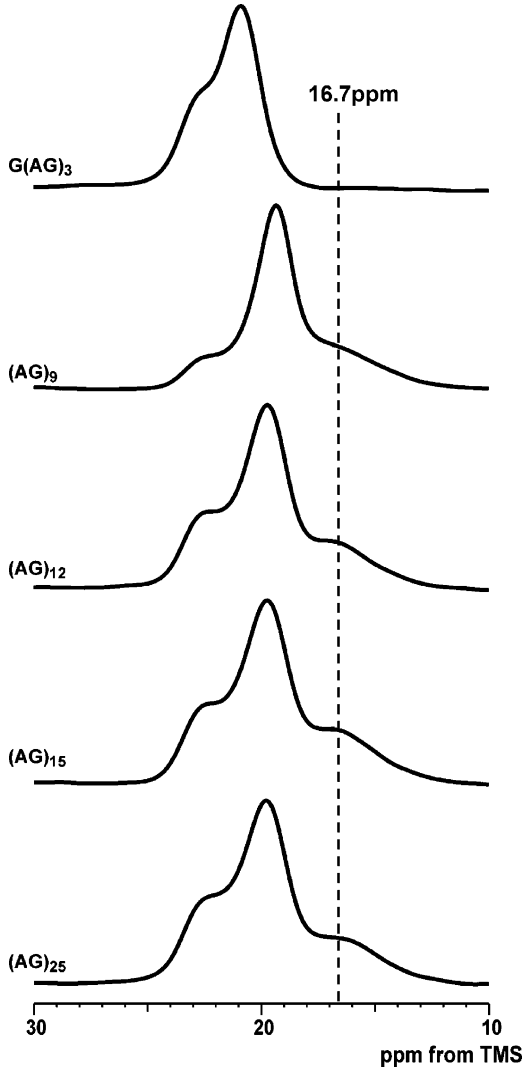

Figure 1. Expanded Ala Cβ peaks of ^{13}C CP/MAS NMR spectra of $G(AG)_3$, $(AG)_9$, $(AG)_{12}$, $(AG)_{15}$, and $(AG)_{25}$.

Results and Discussions

^{13}C CP/MAS NMR Spectra of Alanine-Glycine Oligomers. Figure 1 shows the expanded Ala Cβ region of ^{13}C CP/MAS NMR spectra for a series of $(AG)n$ peptides, $G(AG)_3$, $(AG)_9$, $(AG)_{12}$, $(AG)_{15}$, and $(AG)_{25}$. The Ala Cβ peak of the short peptide, $G(AG)_3$ in the silk II state showed only two peaks at lower field corresponding to the β-sheet peak region and no peak at 16.7 ppm. The broad 16.7 ppm peak which has been assigned to distorted β-turn and/or random coil was observed in longer peptides, $(AG)_n$ ($n = 9$, 12, 15, and 25).[2] The fraction of the intensity of the 16.7 ppm peak for the Ala methyl region was slightly smaller for $(AG)_9$ compared with that for the longer

(13) Asakura, T.; Nakazawa, Y.; Ohnishi, E.; Moro, F. *Protein Sci.* **2005**, *14*, 2654−2657.
(14) Pines, A.; Gibby, M. G.; Waugh, J. S. *J.Chem. Phys.* **1972**, *56*, 1776−1777.
(15) Gullion, T.; Schaefer, J. *Adv. Magn. Reson.* **1989**, *13*, 57−83.
(16) Michal, C. A.; Jelinski, L. W. *J. Biomol. NMR* **1998**, *12*, 231−241.
(17) Kameda, T.; Zhao, C.; Ashida, J.; Asakura, T. *J. Magn. Reson.* **2003**, *160*, 91−96.

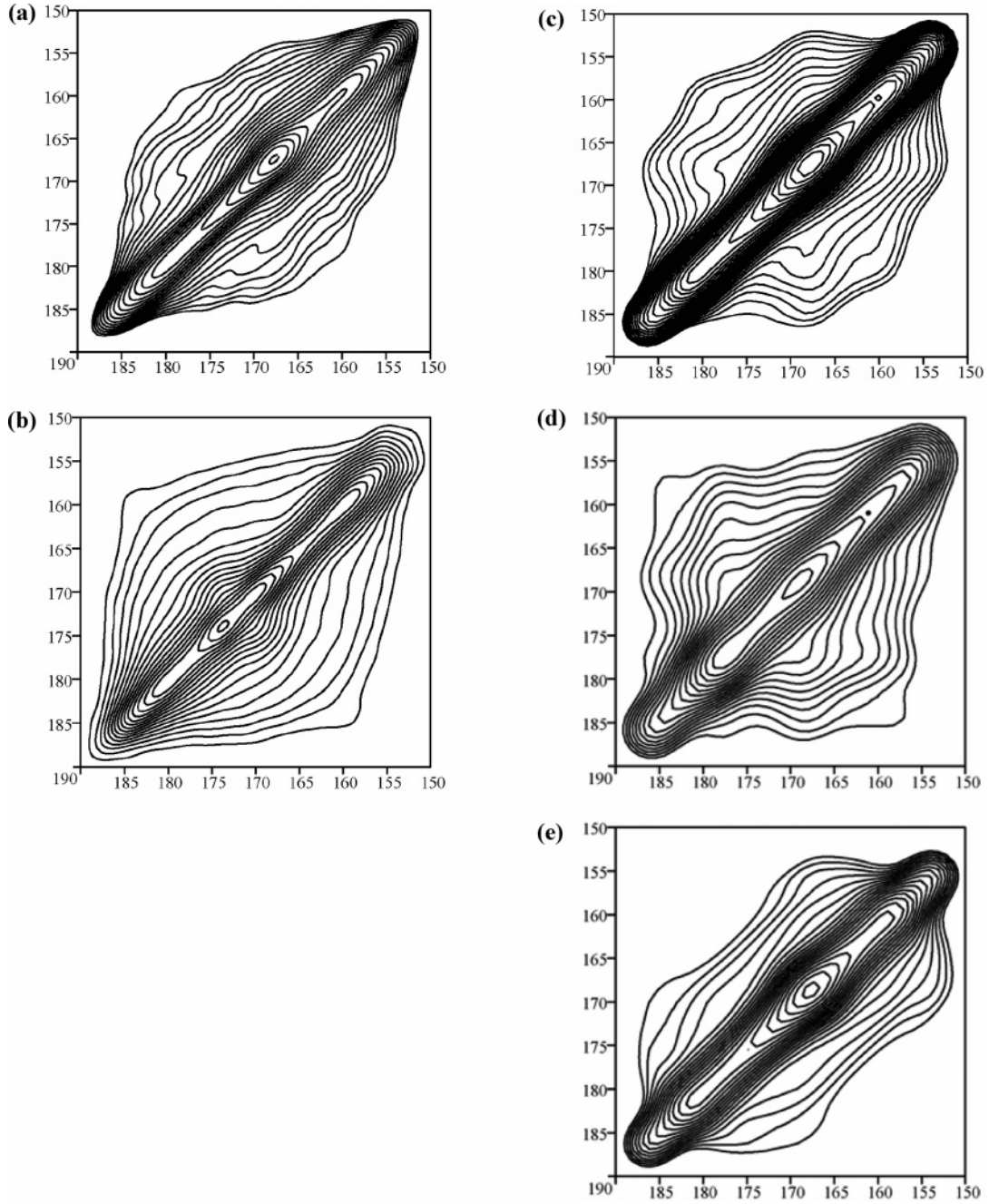

Figure 2. ^{13}C spin diffusion NMR spectra of expanded carbonyl region of (a) $(AG)_6A[1\text{-}^{13}C]G^{14}[1\text{-}^{13}C]A^{15}G(AG)_7$ and (b) $(AG)_8A[1\text{-}^{13}C]G^{18}[1\text{-}^{13}C]A^{19}G(AG)_5$ observed under slow MAS condition. The corresponding simulated spectra (c) and (d) and the calculated spectrum of (e) (antiparallel β-sheet sheet (ϕ and $\varphi = -150°$ and 150°, respectively)) are also shown.

peptides, $(AG)_{12}$, $(AG)_{15}$, and $(AG)_{25}$, the fraction being almost the same in the latter three peptides. These data suggest the appearance of a single unit of new structure in the chain when the length of the oligomer exceeds a critical value. This is compatible with previous evidence[13] for the existence of a lamellar structure in $(AG)_{15}$ obtained by ^{13}C CP/MAS NMR using selective stable isotope labeling.

^{13}C Spin Diffusion NMR Spectra. The ^{13}C spin diffusion NMR spectra of the expanded carbonyl region of (a) $(AG)_6A[1\text{-}^{13}C]G^{14}[1\text{-}^{13}C]A^{15}G(AG)_7$ and (b) $(AG)_8A[1\text{-}^{13}C]G^{18}[1\text{-}^{13}C]A^{19}G(AG)_5$ observed under slow MAS condition are shown in Figure 2 together with the corresponding simulated spectra, (c) and (d), and the calculated spectrum of (e) antiparallel β-sheet sheet (ϕ and $\varphi = -150°$ and 150°). When comparison is made with the calculated spectrum (e) for an antiparallel β-sheet structure, it is obvious that the non-diagonal components in the observed spectra (a) and (b) are more enhanced, suggesting the presence of additional structures to the antiparallel β-sheet structure in the peptide. Figure 2b shows more of the non-diagonal components than Figure 2a.

Figure 3 shows the ^{13}C CP/MAS NMR spectra of (a) $(AG)_7[3\text{-}^{13}C]Ala^{15}G(AG)_7$ and (b) $(AG)_{15}$ with natural abundance, and the difference spectrum (c) = (a) − (b), together with the deconvoluted spectrum (d) of the Ala Cβ region. The deconvoluted Ala^{15} Cβ peaks of $(AG)_7[3\text{-}^{13}C]Ala^{15}G(AG)_7$ yielded 23% *distorted* β-turn (16.7 ppm), 55% β-sheet (alternating Ala residues) (19.1 ppm), and 22% β-sheet (parallel Ala residues) (22.4 ppm) (Figure 3d).[11] It appears that the increased nondi-

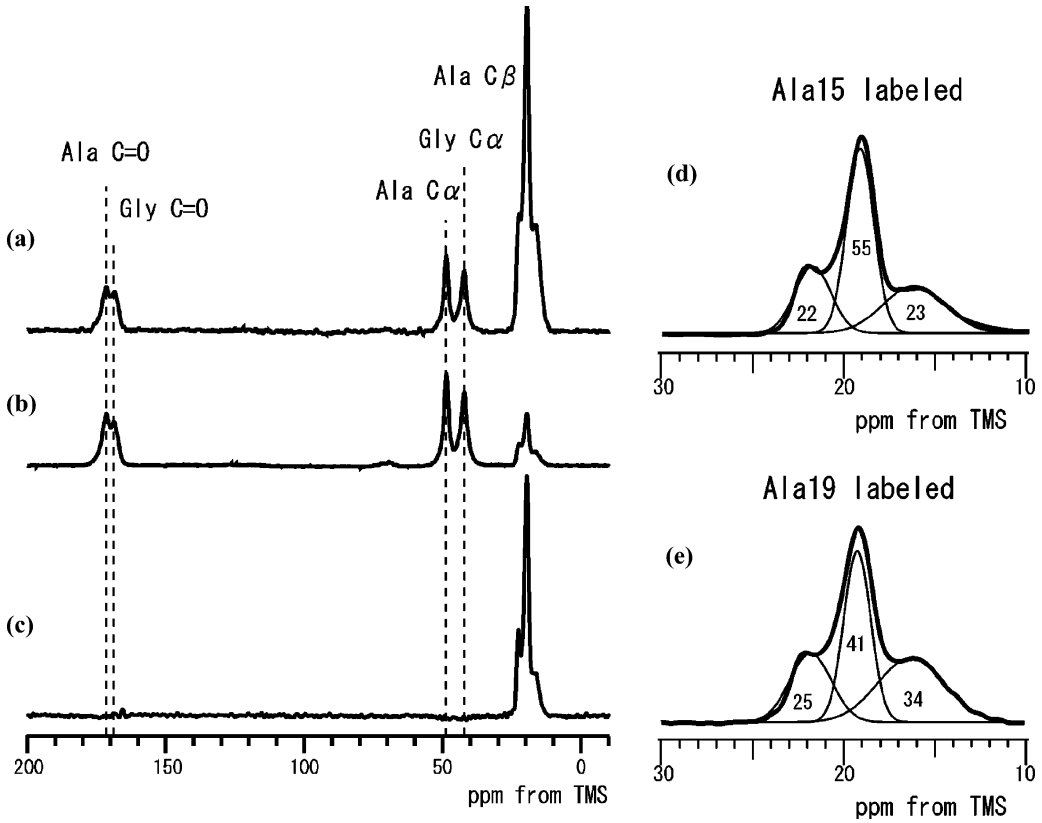

Figure 3. ^{13}C CP/MAS NMR spectra of (a) $(AG)_7$[3-^{13}C]Ala^{15}G$(AG)_7$ and (b) $(AG)_{15}$ from natural abundance, and the difference spectrum, (c) = (a) − (b) along with the deconvoluted spectrum (d) of the Ala Cβ region.

agonal components in Figure 2a are caused by the presence of the *distorted* β-turn together with the antiparallel β-sheet. Figure 3e shows that the deconvoluted Ala^{19} Cβ peaks of $(AG)_9$[3-^{13}C]Ala^{19}G$(AG)_5$ yielded 34% *distorted* β-turn(16.7 ppm), 41% β-sheet (alternating Ala residues)(19.1 ppm), 25% β-sheet (parallel Ala residues)(22.4 ppm), and therefore an increased *distorted* β-turn content compared with the same peptide labeled at Ala^{15} (see Figure 3d). This difference correlates with the increase in the nondiagonal components in Figure 2b compared with that in Figure 2a.

^{13}C spin diffusion NMR spectral patterns were calculated for Ala residues as a function of the torsion angles, ϕ and φ (see Figure S1 in the Supporting Information). It is noted that the patterns change, largely depending on the torsion angles.[3] It is worthwhile to simulate the observed spin diffusion pattern (see a and b of Figure 2). Two peaks observed at the lower field at 19.1 and 22.4 ppm have both been assigned to two different intermolecular arrangements of the antiparallel β-sheet both with the same torsion angles of Ala residue (ϕ and $\varphi = -150°$ and 150°).[11] Therefore, we will concentrate here on the broad 16.7 ppm peak which gives information concerning the distribution of the torsion angles in the distorted β-turn region within one chain. We first simulate the spin-diffusion NMR pattern of $(AG)_6$A[1-^{13}C]G^{14}[1-^{13}C]A^{15}G$(AG)_7$. The ^{13}C chemical shift contour plot of the Cβ carbon of Ala residues as a function of the torsion angles ϕ and φ has been reported previously.[18,19] This has been used to evaluate the distribution of the torsion angles from the chemical shift distribution of the 16.7 ppm peak.[20] Figure 4a shows these chemical shifts as a histogram. Each histogram of the chemical shifts can be converted to the corresponding ϕ and φ torsion angle distribution shown in the same color in Figure 4b. We estimated the pertinent sets of the torsion angles. Thereafter, the corresponding calculated spin diffusion patterns as shown in the Supporting Information were selected. Finally, the spin diffusion spectrum was calculated by taking into account the fraction for each (ϕ, φ) angle in Figure 4. Figure 2c shows the simulated pattern for $(AG)_6$A[1-^{13}C]-G^{14}[1-^{13}C]A^{15}G$(AG)_7$ according to this series of calculations. A comparison shows that the observed spectral pattern (Figure 2a) was well reproduced by the simulated pattern (Figure 2c). A similar simulation was also performed for $(AG)_8$A[1-^{13}C]-G^{18}[1-^{13}C]A^{19}G$(AG)_5$ as shown in Figure 2d. Here the fraction of the distorted β-turn was 34%. The simulated spectrum of A^{19} (Figure 2d) is slightly different from that of A^{15} (Figure 2c), reflecting the increase in the fraction of the distorted β-turn structure. Thus, the difference in the observed spectra between A^{15} and A^{19} peptides with different labeling positions could be well reproduced by the simulated spectra.

REDOR Observation. REDOR experiments of peptides doubly labeled with [^{13}C] and [^{15}N] at different locations are very useful for studying peptide and protein structures containing turns, because the measured atomic distance between C and N nuclei is shortened at the position of the turn.[16] Table 1 compares the observed interatomic distances between the labeling sites determined from REDOR plots (see Figure S2 in the Supporting Information) with predicted averaged interatomic distances taking into consideration the percentage composition of the

(18) Spera, S.; Bax, A. *J. Am. Chem. Soc.* **1991**, *113*, 5490−5492.
(19) Asakura, T.; Iwadate, M.; Demura, M.; Williamson, M. P. *Int. J. Biol. Macromol.* **1999**, *24*, 167−171.
(20) Asakura, T.; Kuzuhara, A.; Tabeta, R.; Saito, H. *Macromolecules* **1985**, *18*, 1841−1845.

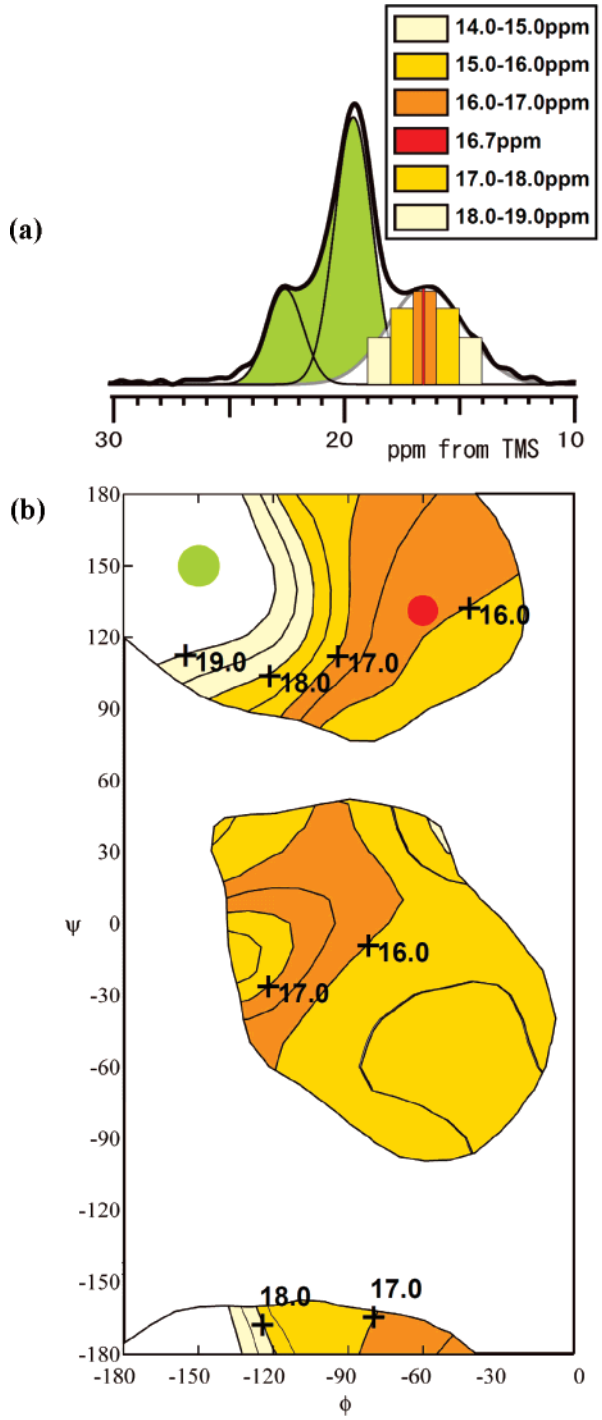

Figure 4. Chemical shift distribution as a histogram (a) in the distorted β-turn peak of $(AG)_6A[1\text{-}^{13}C]G^{14}[1\text{-}^{13}C]A^{15}G(AG)_7$. The ^{13}C chemical shift contour plot (b) of the Cβ carbon of Ala residue was used to evaluate the distribution of the torsion angles from the histogram.

β-turn and β-sheet secondary structures at this location as determined by deconvolution of the Ala Cβ CP/MAS spectra reported previously.[13] If the $(AG)_{15}$ molecule is assumed to take only the β-sheet structure, all the interatomic distances should be longer than the observed distances by REDOR by 0.2−0.3 Å for the peptides D1−D4, and 0.8 Å for D5. By taking into account the presence of the β-turn structure, the predicted distances become closer to, and fairly well correlated with, the observed distances. Thus, the results from REDOR are in good agreement with those from Ala Cβ CP/MAS NMR, providing

Table 1. Atomic Distances Calculated from REDOR Plots for Five $^{13}C,^{15}N$-Labeled Peptides, (D1) $(AG)_7[^{15}N]A^{15}[2\text{-}^{13}C]G^{16}(AG)_7$, (D2) $(AG)_7A[^{15}N]Gly^{16}[2\text{-}^{13}C]Ala^{17}G(AG)_6$, (D3) $(AG)_6A[1\text{-}^{13}C]Gly^{14}A[^{15}N]Gly^{16}(AG)_7$, (D4) $(AG)_7[1\text{-}^{13}C]Ala^{15}G[^{15}N]Ala^{17}G(AG)_6$, (D5) $(AG)_7[^{15}N]Ala^{15}[1\text{-}^{13}C]Gly^{16}(AG)_7$ the Labeling Sites, Atomic Distances by Assuming β-Sheet and β-Turn Together with the Calculated Distances by Assuming the Fraction of 16.7 ppm Peak Are Listed

	labeled site	observed distances (Å)	β-sheet (Å)	β-turn (Å)	simulated distances (Å)
D1	$[^{15}N]Ala^{15}\cdots[2\text{-}^{13}C]Gly^{16}$	4.6 ± 0.1	4.82	4.74	4.8
D2	$[^{15}N]Gly^{16}\cdots[2\text{-}^{13}C]Ala^{17}$	4.7 ± 0.1	4.96	4.17	4.8
D3	$[1\text{-}^{13}C]Gly^{14}\cdots[^{15}N]Gly^{16}$	4.5 ± 0.1	4.77	3.85	4.6
D4	$[1\text{-}^{13}C]Ala^{15}\cdots[^{15}N]Ala^{17}$	4.5 ± 0.1	4.76	2.94	4.4
D5	$[^{15}N]Ala^{15}\cdots[1\text{-}^{13}C]Gly^{16}$	5.2 ± 0.3	6.02	5.05	5.8

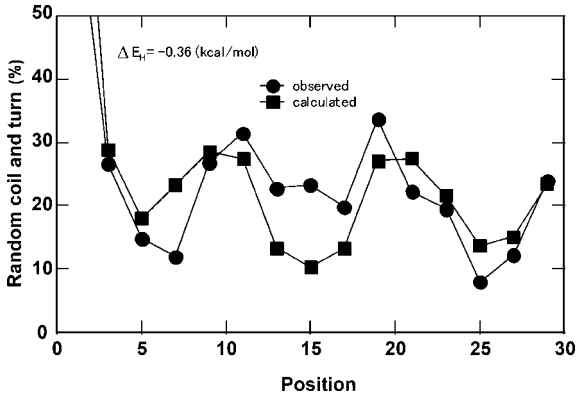

Figure 5. Relative intensity of the 16.7 ppm peak calculated from the deconvolution of Ala Cβ peaks in the ^{13}C CP/MAS NMR spectra of 15 $[3\text{-}^{13}C](AG)_{15}$ with different $[3\text{-}^{13}C]$Ala-labeling sites as a function of the ^{13}C-labeled position. The calculated fractions of random coil and turn (non-β-sheet structure) when $\Delta E_H = -0.36$ kcal/mol using the statistical mechanical method are also shown. Details of the calculation are described in the text.

strong supporting evidence for the existence of a combination of β-turn and β-sheet secondary structure at Ala^{15} in $(AG)_{15}$.

Statistical Mechanical Calculation. Figure 5 shows that the fraction of the peak at 16.7 ppm increases appreciably at positions 9 and 11. This finding suggests a folded lamellar structure with a β-turn at these positions as estimated from the deconvoluted Ala Cβ peaks in Figure 3. The decreased fractions after the 11th position remain unchanged until the 17th position, and the fraction reaches the next maximum at the 19th position. Thereafter, the fraction decreases to the minimum at the 25th position and approaches the maximum again at the final 29th position (C-terminus). Interestingly, it appears that such changes in the fraction of the peak at 16.7 ppm indicate the presence of lamellar structure, as discussed in the previous paper.[13]

In order to reproduce the distribution of turns along the peptide shown in Figure 5, we used statistical mechanical calculations[21] to search for the most probable structure for $(AG)_{15}$, possessing either one or two β-turns at different positions along the peptide. These calculations were based on the following assumptions:

(1) After β-turn formation along the chain, there is at least one pair of the intramolecular hydrogen-bonded strands forming a β-sheet structure. Therefore, among Ala residues, the first

(21) Flory, P. J. *Statistical Mechanics of Chain Molecules*; John Wiley & Sans, Inc.: New York, 1969.

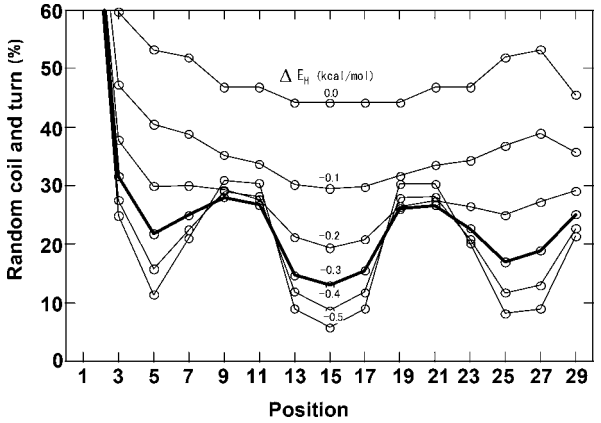

Figure 6. *P*(*j*) plotted against the Ala residue position, *j*, in the $(AG)_{15}$ molecule as a function of ΔE_H (summed stabilization energies (kcal/mol) for the interresidue hydrogen bonds of the residues in the β-sheet structure). The details of the calculation used are described in the text.

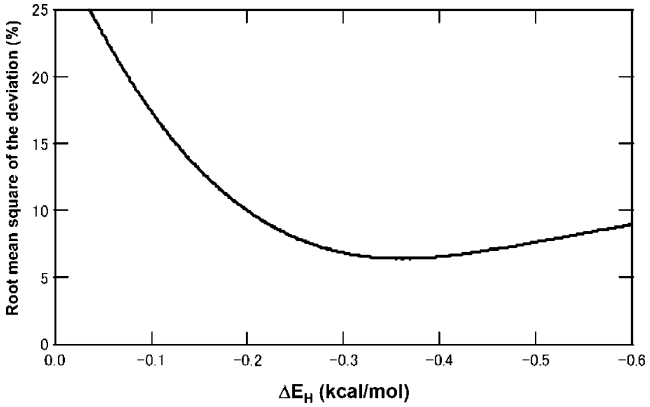

Figure 7. Plot showing how the root-mean-square of the deviation between the fractions of the non-β-sheet conformations obtained experimentally by deconvolution and predicted by statistical dynamics changes in $(AG)_{15}$ as a function of ΔE_H.

residue which can form the β-turn is the third Ala residue, while the 29th Ala is unable to form the β-turn.

(2) The direction of the β-turn formation along the chain is always from the N-terminal to the C-terminal. In addition, to form the hydrogen bonding for the β-sheet structure, the start of the turn is always on an Ala residue with an odd number.

3) There are either one or two turns in the peptide.

Using these assumptions, the 80 possible structures with one or two β-turn positions in one chain were taken into account; see the Supporting Information for the further details, Figure S3. The occurrence probability, $p(i)$, of the ith structure for $(AG)_{15}$ was calculated as

$$p(i) = \exp(-\Delta E(i)/kT)$$

where $\Delta E(i)$ is the potential energy of the ith structure, k is the Boltzmann's constant, and T is the absolute temperature. If the stabilization energy, ΔE_H, due to formation of interresidue hydrogen bonds for each residue with β-sheet structure is assumed to be dominant, the relative potential energy of the ith structure, $\Delta E(i)$, with the occurrence probability, $p(i)$, is calculated as

$$\Delta E(i) = n(i)\Delta E_H$$

where $n(i)$ is number of the residue with such a relative stabilization energy in the ith structure. Then the occurrence probability, $P(j)$, where the Ala residue j in the $(AG)_{15}$ molecule is *not* involved in intermolecular hydrogen-bonding formation within a β-sheet structure is calculated as[21]

$$P(j) = \sum \delta(ij) \exp(-n(i)\Delta E_H/kT) / \sum \exp(-n(i)\Delta E_H/kT)$$

where $\delta(ij) = 0.0$ when the Ala residue j in the ith structure is involved in the interresidue hydrogen bonds with β-sheet structure, while $\delta(ij) = 1.0$ when the Ala residue j in the ith structure is not involved in the interresidue hydrogen-bonding formation with β-sheet structure. The $P(j)$ was calculated as a function of ΔE_H (0.0, −0.1, −0.2, −0.3, −0.4, −0.5 kcal/mol: 1 cal = 4.183 joules). The larger absolute value of ΔE_H means that the contribution of the interresidue hydrogen bonds with β-sheet structure to the potential energy of the chain becomes larger. Figure 6 shows $P(j)$ plotted against the Ala residue position, j, in the molecule. The following points arise from Figure 6: (1) When $\Delta E_H = 0.0$ kcal/mol, the 80 different structures have the same occurrence probabilities. In this case, the central residues which tend to be incorporated into the β-sheet structure have higher occurrence probability, and therefore the fraction of the residues which do not contribute to the β-sheet becomes smaller. Thus, the plot becomes a shallow line when $\Delta E_H = 0.0$ kcal/mol.

(2) The plots are markedly asymmetric because the N-terminal Ala residue cannot contribute to β-sheet formation, but the 29th Ala residue just before C-terminal Gly residue can participate in a β-sheet.

(3) With increasing ΔE_H, the center of the plot initially becomes deeper and then two maxima appear when $\Delta E_H < -0.3$ kcal/mol. Thus, the observed percentage β-sheet content at different points along the peptide determined by deconvoluting Ala Cβ peaks in the ^{13}C CP/MAS NMR spectra (Figure 5) could be reproduced for $\Delta E_H < -0.3$ kcal/mol. Figure 7 shows how the root-mean-square of the deviation between the observed fractions of non-β-sheet conformations determined by deconvolution and the predicted fractions calculated using statistical mechanics changes with ΔE_H between 0.0 and −0.6 kcal/mol. The minimum deviation was obtained at $\Delta E_H = -0.36$ kcal/mol although the shape of the line is shallow to the right of the minimum. The fraction of non-β-sheet conformations calculated for $\Delta E_H = -0.36$ kcal/mol was plotted against the position in Figure 5. There is a qualitative agreement between the observed and calculated plot although any intermolecular interactions are not taken into account in the calculations. We propose the five closely similar structural models (a−e) with high occurrence probabilities ($p \geq 0.10$) for $\Delta E_H = -0.36$ kcal/mol (see Figure S4 in the Supporting Information). Each model contains two β-turn structures. The turn positions are (7,19), (9,19), (9,21), (11,21), and (11,23). These structures form 16 β-sheet hydrogen bonds in one peptide, the largest possible number in this analysis, and therefore are considered to have the highest stabilities as well as the highest occurrence probabilities. The presence of these five closely related structures is likely to contribute to the increase in the number of β-turns in Figure 5. The average length of the strands is calculated to be 11.2 amino acid residues and 6.98 (χ value) × 11.2/2 = 39.1 Å. Thus, the combination of a statistical mechanical analysis with experimental approaches based on advanced solid-state NMR methods provides a powerful tool to examine the detailed structure of

silk peptides. It will be of interest to apply this tool to larger peptides taken from silk sequences taken from a range of lepidopterans to discover more about lamellar structures in silks.[22]

Acknowledgment. T.A. acknowledges Dr. D. Knight (Oxford University) and Dr. Hajime Saito for stimulating discussions. Dr. Jun Ashida (Varian Technologies Japan) is also acknowledged for his useful suggestions about solid-state NMR measurements. T.A. also acknowledges support from the a Grant-in-Aid for Scientific Research from the Ministry of Education, Science, Culture and Sports of Japan (18105007).

Supporting Information Available: Additional Information as noted in the text. This material is available free of charge via the Internet at http://pubs.acs.org.

JA070128H

(22) Dicko, C.; Kenney, J. M.; Vollrath, F. *Adv. Protein Chem.* **2006**, *73*, 17−53.